0273-2289/91/2829—0685$02.80

Modeling of an Immobilized-Cell Three-Phase Fluidized-Bed Bioreactor

JAMES N. PETERSEN*,[1] AND BRIAN H. DAVISON[2]

[1]Chemical Engineering Department, Washington State University, Pullman, WA 99164-2710; and [2]Chemical Technology Division, Oak Ridge National Laboratory, Oak Ridge, TN 37831-6226

ABSTRACT

A mathematical model of a three-phase, tapered, fluidized-bed bioreactor has been developed. This model includes the effects of the tapered bed, a variable dispersion coefficient, and the concentration profile inside the biocatalyst bead on the reaction rate within the bed. Parameters in this model were obtained by adjusting them, within a realistic range, such that the square of the difference between the values predicted by the model and those obtained experimentally was minimized. The model was found to predict experimentally obtained concentration profiles quite accurately. It also demonstrates the need to include the effects of variable dispersion in three-phase systems where the gas phase is being generated inside the reactor, as the dispersion coefficient varied by more than an order of magnitude across the bed.

Index Entries: Fluidized-bed; immobilized-cell; variable dispersion; three-phase.

INTRODUCTION

A key element in the development of advanced bioreactor systems capable of very high conversion rates is the retention of high concentrations of the biocatalyst within the bioreactor. At the same time, the reaction environment must ensure that the substrate is in intimate contact with the biocatalyst. One very effective method of achieving these goals is by immobilizing the biocatalyst into a well-defined matrix. Then, this

*Author to whom all correspondence and reprint requests should be addressed.

immobilized biocatalyst can be placed into a reaction environment that provides effective mass transport, such as a fluidized bed. Previous studies have shown that such systems may be more than ten times as productive as conventional technology (*1*).

Previously, various models have been developed for studying fixed- and fluidized-bed bioreactors (FBRs). Of these, many have considered only two-phase (liquid–solid) systems. For example, Moynihan et al. (*2*) studied urea hydrolysis by urease that was immobilized onto a fixed bed of ion-exchange resins. They used a modified Michaelis-Menten rate expression to describe the reaction kinetics. Ionic equilibria of product and buffer species were included to account for pH changes generated by reaction. They developed an isothermal, heterogeneous plug-flow model, using an effectiveness factor to describe the reaction-diffusion process within the particle phase.

Park et al. (*3*) developed a model for a three-phase (gas–liquid–solid), fluidized-bed bioreactor for penicillin production. However, they considered only the limiting cases of complete mixing and plug flow. Recently, Wisecarver and Fan (*4*) presented a model for biological phenol degradation that used double-substrate-limiting kinetics. The model they presented included the effects of gas–liquid and liquid–solid mass transfer, axial dispersion of the liquid phase, and simultaneous diffusion and reaction within the biofilm. However, they assumed that the solids were well mixed and steady-state growth conditions were maintained, implying that the concentration on the surface of the biofilm was constant throughout the reactor. These assumptions, together with the assumption that the axial dispersion coefficient was constant throughout the reactor, allowed them to develop an analytical solution for the bulk fluid concentration as a function of the surface phenol concentration. They then calculated the concentration profile through the biofilm to determine the surface concentration. Then, using material balance information, they determined the reactor exit concentration.

Hamamci and Ryu (*5*) presented a model of a three-phase, fluidized-bed bioreactor. Although they performed their studies using a tapered-bed reactor, they did not include this information in the differential equations they presented. In addition, they assumed that the dispersion coefficient was constant throughout the bed. Gòdia et al. (*6*) used a tanks-in-series model to describe ethanol production in a packed bed. They included the intrinsic reaction kinetics, the external mass transfer, and internal diffusion-reaction within the gel beads. Although the tanks-in-series model can accurately predict the end points of the system, it is difficult to draw definitive conclusions about the concentration profile in the reactor bed.

In this article, a new model of an immobilized-cell, fluidized-bed bioreactor is presented. In this reactor, *Zymomonas mobilis* was immobilized and used to convert glucose to ethanol and CO_2. Because, in addition to the desired product, ethanol, this system also produces CO_2 gas at high

rates, a three-phase reaction system results (solid biocatalyst, liquid solution of substrate and product, and gaseous CO_2). Previous research (*7*) has shown that the degree of back-mixing in such reactors is a function of the gas flow rate through the bed. Since CO_2 is being produced in the reactor, a dispersed plug-flow model with a variable dispersion coefficient is used to describe the bed hydrodynamics. The effectiveness factor was calculated to account for the effects of concentration profiles within the biocatalyst bead.

MATERIALS AND METHODS

The system that the model was to describe consisted of a three-phase, fluidized-bed bioreactor, in which biocatalyst particles were suspended by the upward flow of liquid and gas. Inocula of *Z. mobilis* NRRL-B-14023 were used and grown in still Fernback flasks containing 50 g/L glucose and 5 g/L yeast extract (DifCo). This strain has been used previously at ORNL and is a rapid fermentor of the desired media. The inocula were centrifuged to concentrate the cells before adding them to the gelling solution; the final gel concentration was 4% κ-carrageenan. Iron oxide (3%) was sometimes added to the gel to increase the specific density. The bead production technique has been described in detail elsewhere (*8*). In brief, the gel was extruded as a jet under an imposed vibration dispersing the jet into small monodispersed droplets that were stabilized in a 0.3*M* KCl solution. The bead diameters were measured visually and were made to be smaller than 2 mm. The synthetic laboratory medium was composed of the desired concentration of refined glucose, 0.5% yeast extract, and 0.1*M* KCl.

The fermentations were performed in a tapered reactor (92.7 cm in length with an ID uniformly tapered from 1.27–3.81 cm). Above the bed, an expansion section (7.62-cm ID) was provided to allow the biocatalyst beads to fall back into the column. The liquid was removed by overflow in a sidearm settling chamber. This reactor is shown schematically in Fig. 1. The temperature was controlled at 30°C by a jacketed water bath. The pH was controlled (generally at pH 5) by the addition of KOH at multiple axial ports along the FBR. The gas produced was vented out the top of the column and measured in a wet-test meter as the volumetric rate of CO_2 production.

Samples were taken from all ports of the reactor simultaneously, quickly filtered, and frozen for later analysis. The glucose concentration was determined using a YSI model 27 Industrial Analyzer. The ethanol concentration was measured by gas chromatography on a Chromosorb 101 column at 150°C with an FID. Cell concentrations were determined microscopically in a counting chamber for both beads and the broth. Periodically, some beads were removed, patted dry, and dissolved to a 100-fold dilution in distilled water, and the cell number was counted.

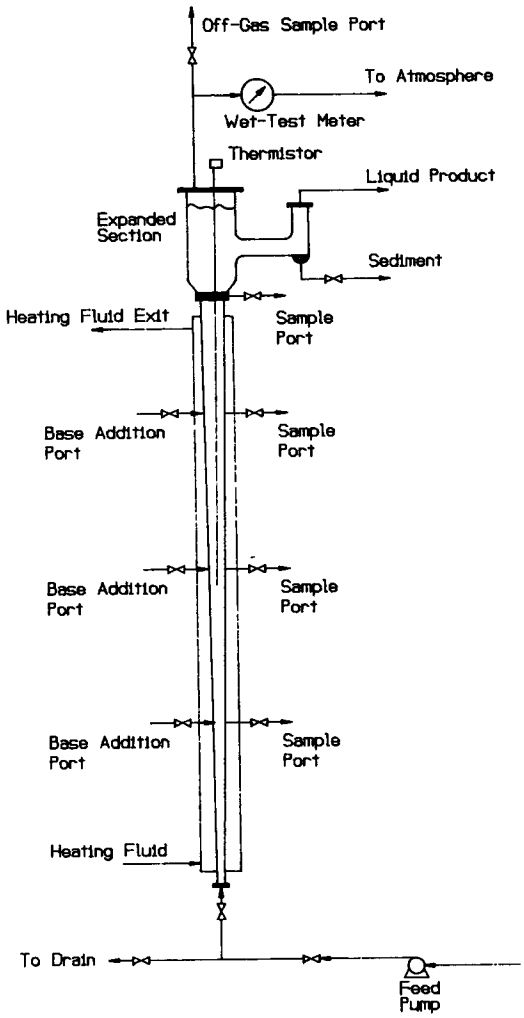

Fig. 1. Schematic diagram of the fluidized bed bioreactor.

MODEL DEVELOPMENT

An effective model of this system must account for the reaction kinetics employed by the biocatalyst, the transport phenomena used to move species into and out of the biocatalyst bead, and the hydrodynamics of the fluidized bed. In the following sections, each of these topics will be addressed.

Reaction Kinetics

Assuming that the immobilized cell employs the same mechanisms to convert the substrate to products as are used by the free cell, then

Table 1
Parameter Values for the Kinetic Model

Parameter	Description	Value
P_i	Threshold ethanol concentration for ethanol production	55 g/L
P_m	Maximum ethanol concentration for ethanol production	127 g/L
$(q_p)_m$	Maximum specific ethanol production rate	5.0 g/g·h
K_s	Substrate limitation constant for ethanol production	0.5 g/L
K_i	Substrate inhibition constant for ethanol production	500 - 2000 g/L
$Y_{p/s}$	Ethanol yield	0.48 g/g

kinetics developed for free cells can also be used to describe the reaction in this system. Sakaki et al. (*9*) have shown that the rate of reaction for free cells will, in fact, give a good estimate of the overall reaction rate for immobilized *Z. mobilis*.

Lee and Rogers (*10*) studied extensively the reaction kinetics employed by *Z. mobilis* to produce ethanol. They reported that the reaction can be described effectively using a modified Monod-type model with substrate and product inhibition. The degree of product inhibition is assumed to be a linear function of the product concentration between lower and upper concentration limits. That is, if the ethanol concentration is lower than the lower limit, then the ethanol does not affect the kinetics of the reaction. Conversely, if the ethanol concentration is greater than the upper limit, then the reaction is effectively quenched. Using this model, which assumes a constant yield coefficient, the rate of glucose consumption is given by:

$$r_A = -\frac{(q_p)_m}{Y_{p/s}} \frac{S}{K_s+S} \frac{K_i}{K_i+S} f_p \, x \tag{1}$$

where

$$f_p = \begin{cases} 0 & \text{for } P \geq P_m \\ 1-\dfrac{P-P_i}{P_m-P_i} & \text{for } P_i \leq P \leq P_m \quad \text{and} \\ 1 & \text{for } P \leq P_i \end{cases} \tag{2}$$

S is the glucose concentration, P is the ethanol concentration and x is the biomass concentration. The other parameters are defined and numerical values given by Lee and Rogers (*10*) are provided in Table 1. Note that Lee and Rogers determined K_i using a batch culture. Thus, because of parametric insensitivity to changes in K_i, they were only able to estimate a range.

The Biocatalyst Bead

Within the biocatalyst bead, the substrate and products are transported by molecular diffusion. In addition, it is here that the biocatalyst actually converts the substrate to products. Thus, the reactions that produce the desired products are not dependent on the bulk fluid concentrations, but rather on the local conditions within the biocatalyst bead. To account for these effects, an effectiveness factor was employed.

The effectiveness factor, η, tells how processes within the bead affect the reaction rate. Generally, η is <1 because reactions usually occur at a slower rate when the substrate concentration is lowered. However, when substrate inhibition exists, as is the case here, η can be >1. Then, as the inhibitory substrate concentration drops within the bead, the reaction rate can increase.

To calculate the effectiveness factor, at each axial-bed bulk concentration, the following boundary value problem was solved:

their respective values in water, a reasonable first approximation for gel immobilization (*11*).

In this analysis, x, the biomass concentration, has been assumed not to be a function of the radial position within the biocatalyst bead. Because of concentration profiles that will exist within the bead, this will not be strictly true. However, since the effectiveness factor was near unity during the initial growth of the biomass (*1*), the growth would have been relatively uniform. Hence, this assumption will give accurate estimates of the actual value.

This set of equations was solved using the software package COLSYS (*12,13*), which implements the method of spline collocation to solve a mixed-order boundary value problem. In our case, we used a seventh-order collocation polynomial within an adjustable number of finite elements. COLSYS adaptively adjusts the location of the elements to achieve the desired solution accuracy.

Bed Hydrodynamics

To determine the concentrations in the bulk fluid as a function of the axial-bed position, the material balance problem, which describes the fluidized bed, must also be solved. An idealized plug-flow (PFR) model and a model consisting of a series of continuous-stirred-tank reactors (CSTRs) were first considered as methods for describing this situation. Both of these representations had serious deficiencies. The PFR model, while being able to provide axial concentration profiles, was not able to represent adequately the experimentally obtained concentration profiles. The tanks-in-series model was able to provide accurate estimates of exit conditions, but was not able to predict axial concentration profiles. Because of the problems associated with these ideal models, a dispersed plug-flow reactor model was developed to describe the bed hydrodynamics.

In developing this model, several factors must be taken into account. First, the reactors that were used to generate experimental data did not always have a constant cross-sectional area. Second, the presence of a gaseous species in the reactor makes the dispersion coefficient a function of axial position. Because CO_2 is generated in the reactor, the dispersion coefficient should be a function of the CO_2 flow rate through the reactor. Previous research performed in this laboratory (*7*) has shown that, as the gas flow rate increases, the dispersion coefficient initially increases rapidly, but then eventually levels off to a new, higher value. This new value may be more than an order of magnitude higher than the value obtained if no gas is present. Since the gas flow rate through the reactor is the result of the amount of CO_2 that has been generated to that point in the reactor, we chose to represent this effect by allowing the dispersion coefficient, Ψ, to be calculated according to

$$\Psi = \Psi_0 + \alpha\left(1 - e^{-\beta CO_2}\right) \tag{7}$$

Accounting for the above factors, the material balance equations, which describe the axial concentration profiles in the FBR, can be derived. For glucose, this equation is:

$$\frac{d^2s}{dz^2} = \frac{L}{\Psi}\left(u_L - \frac{\alpha\beta e^{-\beta CO_2}}{L}\frac{dCO_2}{dz} - \frac{2\Psi\sin(\theta)}{\rho}\right)\frac{ds}{dz} + \frac{L^2}{\Psi C_0}\eta e_s r_A \qquad (8)$$

for the substrate concentration. In this equation, Θ is the angle of inclination of the tapered section of the bed, Ψ is the dispersion coefficient, u_L is the bulk liquid velocity (a function of the axial position), L is the total bed length, z is the dimensionless axial position, ρ is the radius of the bed at z; ϵ_s is the volume fraction solids, and other parameters are as defined above.

The boundary conditions for this equation are typical Danckwerts boundary conditions, modified to account for the fact that the bed may be tapered at the entrance also. Thus,

$$s - \frac{\Psi}{L\left(u_L - \frac{2\Psi\sin(\theta)}{\rho}\right)}\frac{ds}{dz} - 1 = 0 \qquad at\ z=0$$

$$\text{and} \qquad \frac{ds}{dz} = 0 \qquad at\ z=1 \qquad (9)$$

The CO_2 flow rate is obtained by solving a coupled differential equation, assuming that the CO_2 is generated by the reaction and then flows in a plug-flow fashion through the reactor, and that the amount of CO_2 that dissolves in the liquid is estimated to be negligible. The ethanol concentration can be calculated via a simple, algebraic material balance, as was done inside the bead above.

To solve the nonlinear boundary value problem, we again used the COLSYS code, specifying a seventh-order collocation polynomial. The routine used a collocation technique that placed the collocation points in any number of finite elements. The number and location of the elements were adjusted in an adaptive fashion in order to obtain the desired accuracy.

RESULTS AND DISCUSSION

The equations described in the previous section were solved using double-precision calculations. In solving this problem, first the equations to obtain the effectiveness factor as a function of bulk substrate and product concentrations were solved. Then, using these effectiveness factors, the coupled differential equations describing the concentration profiles in the bed were solved.

Table 2
Parameter Values Used in the Simulation

Parameter	Description	Value
Ψ_0	Base value of the dispersion coefficient when no CO_2 is flowing through the column	518. cm^2/h
α	Pre-exponential term in calculation of the dispersion coefficient.	13600 cm^2/h
β	Exponential coefficient in calculation of the dispersion coefficient.	0.0425 h/(g CO_2)
x	Biomass concentration within the gel bead	52.0 g/L
K_i	Substrate inhibition constant for ethanol production.	290. g/L

To match the sets of experimental data, the parameters used to calculate the dispesion coefficient (Ψ_0, α and β), the biomass concentration within the bead (x), and the substrate inhibition constant for ethanol production (K_i) were adjusted. These last two parameters require some additional explanation. The experimental determination of the biomass concentration was subject to large measurement errors, so there was some uncertainty in its value. The experimental values did, however, give us an idea of the permissible range of this parameter. As for the substrate inhibition constant, Lee and Rogers (*10*) expressed uncertainty in the value of this parameter. Thus, we felt that we could allow it to vary somewhat from the values they assigned.

These parameters were adjusted, within a realistic range, such that the square of the difference between the values predicted by the model and those obtained experimentally was minimized. This was accomplished using the generalized reduced-gradient optimization code (*14,15*). The values of these parameters that best fit the experimental data are given in Table 2.

We examined several sets of operating conditions, having a variety of feed flow rates and feed substrate concentrations. Four of the calculated profiles are shown in Fig. 2. We can see that the model represents the experimental data very well. In virtually all of the cases, the model prediction is within the experimental error of the data points.

Observe that, even though the substrate concentration drops dramatically in the entrance region of the columnar reactor, this is not the section where the majority of the reaction occurs. The amount of CO_2 that is flowing past any particular point in the reactor is indicative of the amount of reaction that has taken place to that point. Since this bed is tapered, much of the biomass is located in the top of the bed where the cross-sectional area is largest. Thus, a significant portion of the reaction is taking place in the top part of the reactor.

However, because of the mixing resulting from the CO_2 flow, the top of the reactor is quite well mixed. This concept is verified by the data in

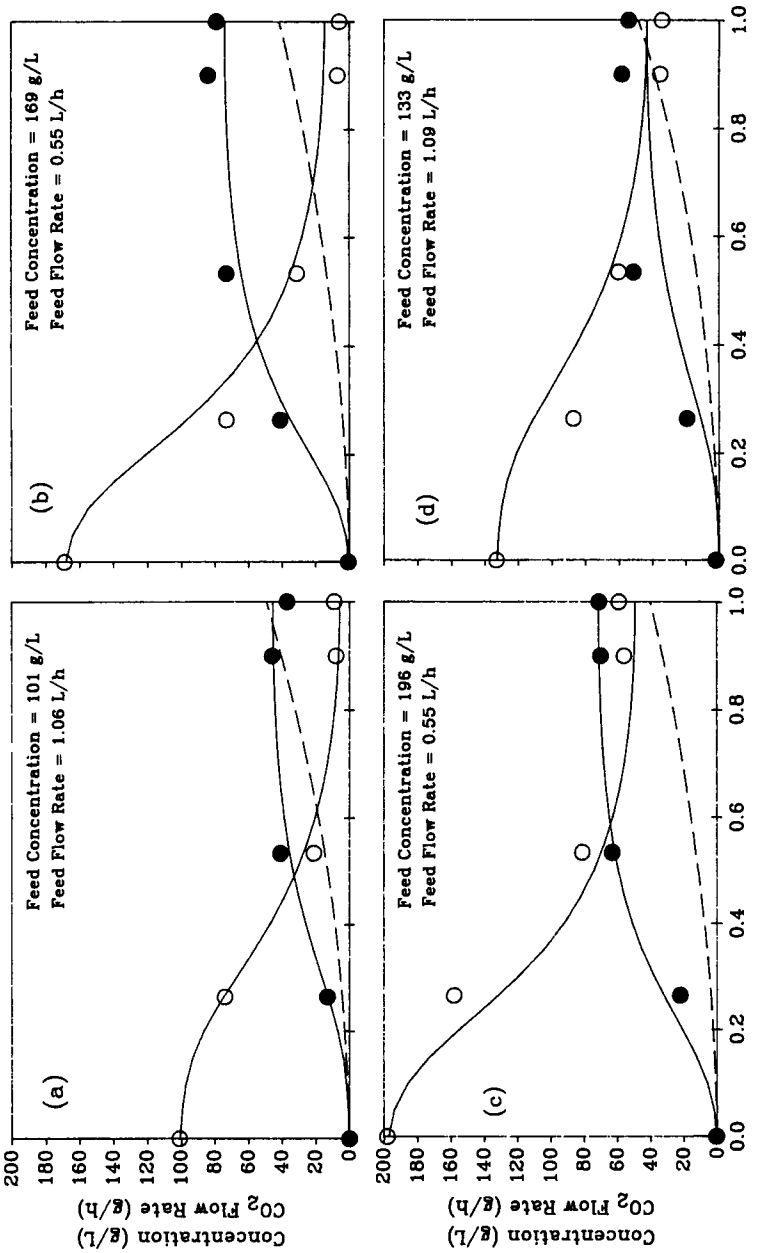

Fig. 2. Experimental and theoretical concentration profiles. The dashed lines show the CO_2 rate. ○ denotes glucose concentrations; ● denotes ethanol concentrations.

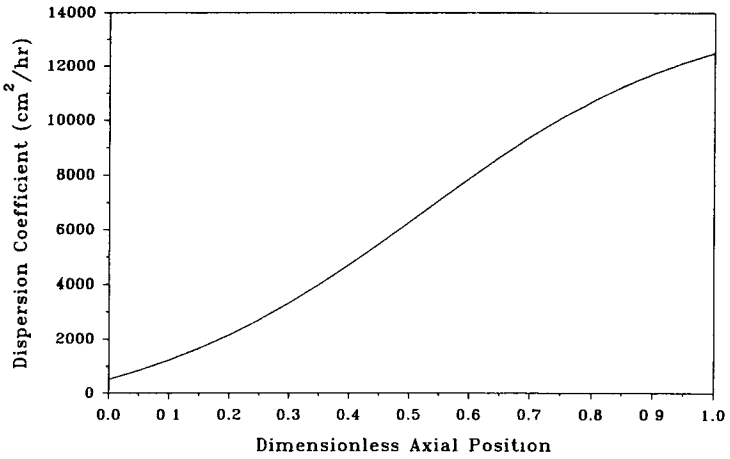

Fig. 3. Dispersion coefficient vs axial position for operating conditions as in Fig. 2a.

Fig. 3, which shows the dispersion coefficient as a function of axial position for the reactor operated as shown in Fig. 2a. First note that the average dispersion coefficient calculated in this case is near the value determined previously (*7*). Also notice that the dispersion coefficient is low near the entrance of the reactor and quite high near the top of the reactor. This means that, because of the mixing produced by the CO_2, the operating mode of the reactor is a function of the axial position. Near the entrance of the reactor, where there is little CO_2 to cause mixing, the reactor is approximately a PFR; near the reactor's exit, where there is a significant CO_2 flow, the reactor is more nearly approximated by a CSTR. Because this portion of the reactor acts as a CSTR, the concentrations of the glucose and ethanol are essentially constant here. However, the bioreaction is still occurring to a significant extent. Based upon these results, we can speculate that the exit substrate concentration could be reduced somewhat if the amount of mixing in the top portion of the reactor could be minimized by, for example, removing much of the CO_2 product gas from the reactor at one or more points.

Although the model was developed for and accommodates a tapered reaction bed, it can also be used to simulate a reactor that has a straight reaction bed. In Fig. 4, the profiles predicted by the model for tapered- and straight-bed reactors are compared. Here, the reactors have the same total reaction volume, and reactor conditions correspond to the case shown in Fig. 2a.

Notice, that, although the profiles are drastically different, the total conversion in each of the reactors is essentially the same since, in this concentration range, the reaction has kinetics that are essentially zero order. Thus, this model would not predict that either of the configurations would be preferential from a conversion standpoint. However, some additional differences are worth examining in more detail.

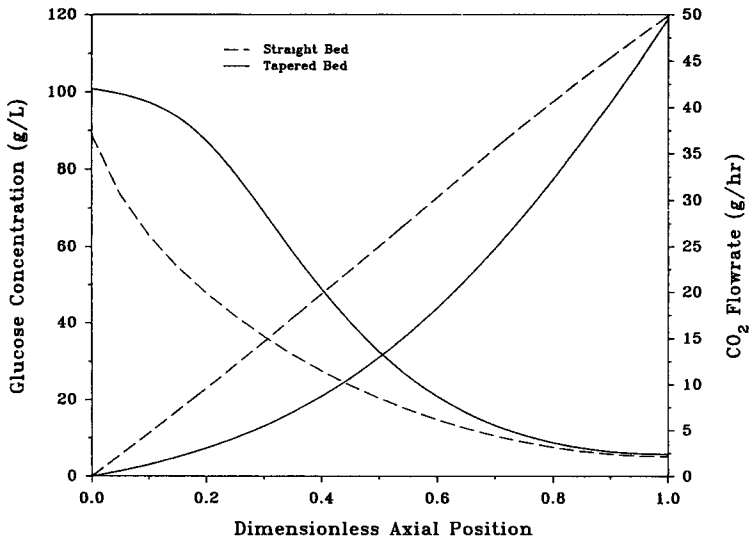

Fig. 4. Predicted profiles for straight and tapered bed reactors.

In the reactor having a straight reaction bed, the biocatalyst will be more or less uniformly distributed along the axial dimension of the reactor. Thus, equivalent amounts of CO_2 are generated at lower axial positions when compared with the tapered bed. This tends to make the glucose and ethanol concentrations more uniform along the length of the reactor.

Because of the Danckwerts boundary conditions given in Eq. 9, the model predicts that, at the entrance of either reactor, the concentration will be lower than the concentration of the feed material. However, in the reactor having a straight bed, this deviation is larger than it is in a tapered bed reactor because of two factors: (1) for the same volumetric feed rate, the bulk fluid velocity at the entrance of the straight bed will be lower than that for the corresponding tapered bed since the cross-sectional area at the entrance of the straight bed is larger than that in the tapered bed; and (2) because more CO_2 is generated at lower axial positions in the straight bed, there is significantly more mixing near the entrance of the straight bed than there is in the tapered bed. Together, these factors cause the substrate concentration at the entrance of the reactor to deviate from the feed concentration more in the straight bed than it does in the tapered bed.

CONCLUSIONS

A mathematical model that describes a tapered, three-phase, fluidized-bed bioreactor has been developed. This model describes the axial concentration profiles observed in an experimental reactor over a wide range of feed flow rates and feed substrate concentrations.

Using this model, we have determined that the CO_2 generated by the microbial reaction causes a great deal of back-mixing in the top portion of the reactor. Also, since the bed is tapered, much of the biomass is located in the top of the bed where the cross-sectional area is largest. Thus, despite the fact that the glucose and ethanol concentrations are essentially constant through this portion of the reactor, the bioreaction is still occurring to a significant extent. If this CO_2 could be removed from the reactor so that it operated in a plug-flow fashion, the exit glucose concentration could be reduced and the exit ethanol concentration could be increased, thus decreasing separation costs.

The model predicts that, on a volumetric basis, the total conversion in the tapered bed will be approximately the same as that which would be obtained for a straight reaction bed. This indicates that, from a conversion standpoint, there is no reason that one configuration is preferable to the other. However, experience has shown that the tapered-bed reactor is considerably easier to operate. The model does, however, predict that the concentration profiles will dramatically differ in the two reactors, primarily because of the different mixing patterns caused by changes in the location at which the CO_2 is generated.

ACKNOWLEDGMENTS

This research was supported by the Office of Energy Utilization Research, Division of Energy Conversion and Utilization, and by the Office of Basic Energy Sciences, Division of Engineering and Geosciences, US Department of Energy, under contract DE-AC05-84OR21400 with Martin Marietta Energy Systems, Inc. Dr. Peterson received sabbatical support from the US Department of Energy Nuclear Energy Research Associates Program administered by Oak Ridge Associated Universities.

REFERENCES

1. Davison, B. H. and Scott, C. D. (1988), *Appl. Biochem. Biotechnol.* **18,** 19–34.
2. Moynihan, H. J., Clark, C. K., and Wang, N.-H.L. (1989), *Biotechnol. Bioeng.* **34,** 951–963.
3. Park, Y. M., Davis, M. E., and Wallis, D. A. (1984), *Biotechnol. Bioeng.* **26,** 457–467.
4. Wisecarver, K. D. and Fan, L.-S. (1989), *Biotechnol. Bioeng.* **33,** 1029–1038.
5. Hamamci, H. and Ryu, D. D. Y. (1987), *Biotechnol. Bioeng.* **29,** 994–1002.
6. Gòdia, F., Casas, C., and Solà, Ç. (1987), *Biotechnol. Bioeng.* **30,** 836–843.
7. Davison, B. H. (1989), *Appl. Biochem. Biotechnol.* **20/21,** 449–460.
8. Scott, C. D. (1987), *Ann. NY Acad. Sci.* **501,** 487–493.
9. Sakaki, K., Nozawa, T., and Furusaki, S. (1988), *Biotechnol. Bioeng.* **31,** 603–606.

10. Lee, K. J. and Rogers, P. L. (1983), *Chem. Eng. J.* **27,** B31–B38.
11. Scott, C. D., Woodward, C. A., and Thompson, J. E. (1989), *Enzyme Microb. Technol.* **11,** 258–263.
12. Ascher, U., Christiansen, J., and Russel, R. D. (1979), *Math. Comput.* **33,** 659–679.
13. Ascher, U., Christiansen, J., and Russel, R. D. (1981), *ACM TOMS* **7,** 209–222.
14. Lasdon, L. S. and Waren, A.D. (1986), *GRG2 User's Guide,* University of Texas, Austin.
15. Edgar, T. F. and Himmelblau, D. M. (1988), *Optimization of Chemical Processes,* McGraw-Hill, New York.